

Evidence for Different Proton and Neutron Deformations in Heavy Nuclei Deduced from Polarized-Deuteron Scattering

H. Clement, R. Frick, G. Graw, F. Merz, H. J. Scheerer,^(a)

P. Schiemenz, N. Seichert, and Sun Tsu Hsun

Sektion Physik, Universität München, D-8046 Garching, West Germany

(Received 3 December 1981)

Inelastic scattering of vector polarized deuterons near $E_d = 20$ MeV has been measured for a series of target nuclei ranging from the sd shell to ^{232}Th . Isoscalar transition rates deduced from a collective-model analysis are found to be in agreement with the corresponding electromagnetic quantities for the quadrupole and octupole excitations of $T = 0$ nuclei and of ^{208}Pb . For the quadrupole excitation in ^{144}Sm , ^{152}Sm , ^{154}Sm , and ^{232}Th about 20% smaller values are obtained, which imply a larger proton than neutron deformation for these nuclei.

PACS numbers: 21.10.Ft, 24.70.+s, 25.50.Dt

The collective model for strongly excited low-lying states correlates the transition strengths with static and dynamic deformations of the nuclear shape. It is surprisingly successful in describing various aspects of the electromagnetic excitation such as transition strengths and static quadrupole moments; even the radial shapes of the collective transition form factors have been established experimentally by inelastic electron scattering experiments.¹ The comparison of electromagnetic and hadronic features of the nuclear excitation offers the possibility to search for differences between charge and mass distributions. In fact, density-dependent Hartree-Fock calculations predict different proton and neutron deformations. Very recently experimental evidence for neutron-proton differences has been reported² for quadrupole excitations of light mirror nuclei in single-closed-shell nuclei, where the shell structure plays an obvious role. For nuclei in the well-deformed regions, where collective models are especially applicable, no such differences have been established so far.

In this Letter we report on a systematic study of inelastic deuteron scattering on selected nuclei ranging from the sd shell up to the actinide region. As a result of their isoscalar character deuterons test the mass distribution of nuclei. The use of polarized particles enables us to project out the details of the diffraction pattern, thus supplying a detailed knowledge³ about the mechanism of the excitation process and the structure of the excited levels. The measurements on ^{16}O , ^{18}O , ^{24}Mg , ^{28}Si , ^{32}S , ^{36}Ar , ^{40}Ca , ^{54}Cr , ^{144}Sm , ^{152}Sm , ^{154}Sm , ^{208}Pb , and ^{232}Th have been performed with the Munich MP tandem accelerator at incident deuteron energies between 18 and 23 MeV. For each target data were taken

for 20–33 angles ranging from 10° up to 160° . For ^{154}Sm and ^{232}Th the quadrupole-triple-dipole magnetic spectrograph has been used in order to separate elastic and inelastic scattering up to very forward angles with an energy resolution of 7 keV. Figure 1 shows as an example the scattering data for the ground-state rotational band in ^{232}Th . In the angular distributions of the differential cross section $\sigma(\theta)$ the diffraction pattern is strongly damped and hardly visible, whereas it shows up very clearly in the vector analyzing power $iT_{11}(\theta)$.

The analyses have been performed⁴ in the framework of the coupled-channels (CC) formalism under the assumption that the collective excitations

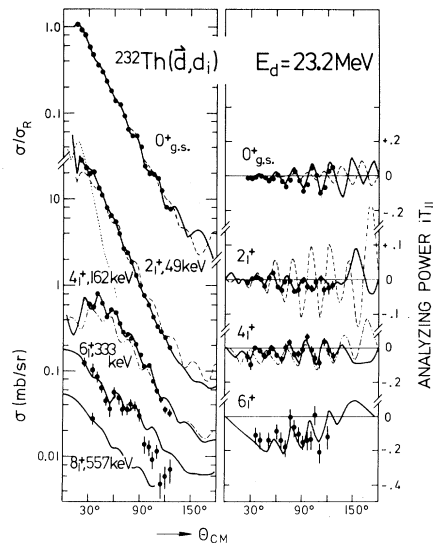


FIG. 1. Vector analyzing power $iT_{11}(\theta)$ and differential cross section $\sigma(\theta)$ for the excitation of the ground-state rotational band in ^{232}Th . The curves drawn are explained in the text.

arise from a deformation of the nuclei. The spherical part of the deuteron-nucleus interaction is described by the global optical potential set of Daehnick, Childs, and Vrcelj,⁵ which reasonably resembles folding expectations. The inelastic form factors

$$f_\lambda(r) = \sum_\mu (1 + \delta_{\mu 0})^{-1} \int V(r, R) (Y_{\lambda\mu} + Y_{\lambda\mu}^*) d\Omega$$

result from the deformation of the nuclear surface which is parametrized according to $R(\theta, \varphi) = R_0 [1 + \sum_{\lambda\mu} \alpha_{\lambda\mu} Y_{\lambda\mu}(\theta, \varphi)]$ and which leads to the nonspherical parts in the deuteron-nucleus interaction $V(r, R(\theta, \varphi))$. The deformation parameters of the individual parts of the optical potential are correlated to each other by the constraint of a constant deformation length, implying that the deuteron-nucleus interaction is dependent on the distance from the nuclear surface. Since the actual projectile-nucleus interaction is nonlocal, phenomenological optical potentials have to be reinterpreted as local equivalent potentials. To account properly for this effect in the CC calculations we have applied the nonlocality corrections according to the prescription of Perey and Austern.⁶ The multipole moments q_λ of the interaction potential are deduced from the inelastic form factors by

$$q_\lambda = \frac{\int r^\lambda f_\lambda(r) r^2 dr}{(4\pi)^{1/2} \int f_0(r) r^2 dr},$$

where the denominator gives the normalization by the volume integral of the interaction. Contrary to the case for heavy ions, the deuteron optical potential is still transparent enough to allow the scattering data to probe the form factors over the relevant radial range. For ¹⁴⁴Sm, e.g., a notch at $r = \frac{2}{3}R_0$ (i.e., on the inner side of the surface-peaked form factor) changing $|q_\lambda|^2$ by 3% also scales the calculated cross section by about the same amount.

To our knowledge this is the first systematic study which uses a global description for the projectile-nucleus interaction to reproduce simultaneously elastic and inelastic scattering over a wide range of nuclear masses. By this procedure we are able to compare systematic trends in the results of inelastic scattering analyses, which are not perturbed by fitting optical-model parameters to each individual nucleus. In fact our CC descriptions for elastic and inelastic scattering are for most of the nuclei as good as descriptions with fitted potentials. The solid lines in Fig. 1 represent the result of the CC analysis, describing ²³²Th as a prolate rigid rotor with a small

positive hexadecapole deformation. In fact the rigid-rotor assumption gives an excellent description for both observables for all states up to the 6⁺. The high sensitivity of the analyzing power to interference terms in the scattering process enables us to draw clear conclusions on the sign of the β_2 and β_4 deformations. The dashed lines show for the 0⁺ and 2⁺ state the effect of changing the sign of β_2 ; the dash-dotted lines show for the 4⁺ state the corresponding effect of the sign change in β_4 . Both changes lead to drastic effects in the analyzing powers. A detailed discussion on the interference terms in the scattering process with an emphasis on the sensitivity to static moments will be given elsewhere.⁷ Since for the 2⁺ scattering on heavy nuclei Coulomb excitation plays an important role in the forward angular region of the cross section (dotted line in Fig. 1: pure Coulomb excitation), we have treated this accurately in all calculations⁴ by using⁸ the results from electron scattering for $B(E\lambda)$ values and charge distributions. The CC analyses of the measurements on the other nuclei reproduce the data for σ and iT_{11} with a similar quality as for ²³²Th. The details of these analyses will be the topic of a forthcoming paper.

Our results for the quadrupole and octupole isoscalar rates $B(IS\lambda)$ for the excitation of the lowest lying 2⁺ and 3⁻ states are compared in Fig. 2 with the corresponding $B(E\lambda)$ values.⁹ The isoscalar rates are derived from the multipole mo-

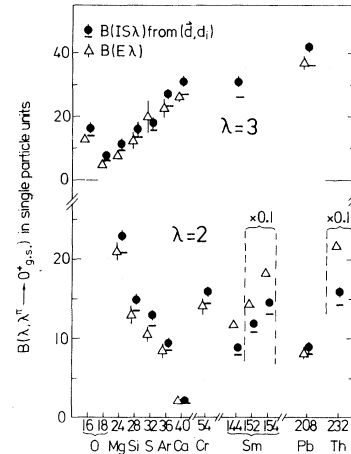


FIG. 2. Isoscalar transition rates for the excitation of the lowest lying 2⁺ and 3⁻ states from (d_{pol}, d_1), in comparison with electromagnetic transition rates (Ref. 9). Horizontal bars indicate a reduction of our values due to the density dependence as discussed in the text (10% for $\lambda = 2$ and 15% for $\lambda = 3$).

ments q_λ of the real central part of the interaction potential by $B(IS, 0^+ \rightarrow \lambda^\pi) = (Zq_\lambda)^2$, where the multiplication by the charge number Z is chosen for direct comparison with $B(E\lambda)$ values. According to Mackintosh¹⁰ these potential moments q_λ are identical to the moments of the mass distribution if the real central part of the optical potential we use can be derived in principle from folding the matter distribution with a density-independent nucleon-projectile interaction. In fact, a realistic interaction is density dependent, causing the q_λ to be slightly larger than the true mass moments. If we assume in a conventional *Ansatz* that the density-dependence has the form $(1 - \gamma\rho^{2/3})$ and take a standard value¹¹ of $\gamma \approx 2 \text{ fm}^{-2}$, we calculate these corrections to be of the order of 5% for the quadrupole moments. Equal multipole moments for charge and mass distributions are expected for $T=0$ nuclei and for ^{208}Pb .¹² Therefore, our results for these nuclei should be about 10% larger than the corresponding electromagnetic values, which in fact is the case for both $\lambda=2$ and $\lambda=3$ (see Fig. 2). For the nuclei in the rare-earth and actinide regions, however, we get values for $B(IS2)$ which are 15%–25% smaller than the corresponding $B(E2)$ values. Since we used for the analysis of these nuclei exactly the same potential set as for all the other nuclei, we are led to the conclusion that for the Sm isotopes and for ^{232}Th the quadrupole mass deformations are substantially smaller than the charge deformations. This observation is independent of the special choice of the interaction potential; the use of other global sets¹³ parametrized with a Woods-Saxon geometry leads to the same findings. We also investigated the possible influence of rearrangement collisions on the inelastic excitation. Coupling the $(d, p)(p, d)$ process, e.g., to the 2^+ excitation in ^{144}Sm causes, however, only negligible changes in the 2^+ observables.

In the case of ^{144}Sm our result for the 2^+ excitation is very plausible in view of the closed neutron shell in this nucleus. Quantitatively it is in full agreement with a theoretical prediction² for the ratio of the neutron to proton moments $M_n/M_p = 0.96$, which has to be compared to the simple collective-model prediction of $N/Z = 1.32$. We obtain a value of $M_n/M_p = 0.93 \pm 0.06$, where the correction for the density dependence is included.

For the strongly deformed nuclei ^{154}Sm and ^{232}Th our results are compared in Fig. 3 with $B(E\lambda)$ values^{9,14} obtained from Coulomb excita-

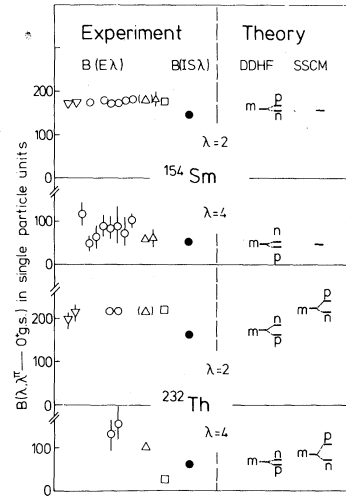


FIG. 3. Quadrupole and hexadecapole transition rates in ^{154}Sm and ^{232}Th . Our results (closed circles) for the isoscalar rates are compared with experimental $B(E\lambda)$ values (Refs. 9 and 14) from lifetime (inverted triangles), Coulomb excitation (open circles), electron scattering (triangles), and μ -atom (squares) measurements and with theoretical results from microscopic calculations (Refs. 15–17) of transition rates from proton (p), neutron (n), and mass (m) moments.

tion, electron scattering, μ -atom, and lifetime studies, as well as with theoretical predictions from density-dependent Hartree-Fock (DDHF) calculations¹⁵ and the Strutinsky shell correction method (SSCM).^{16,17} Experimentally, for $\lambda=2$ transitions the situation seems to be rather clear, whereas for $\lambda=4$ transitions a rather large scatter and large uncertainties in the Coulomb excitation results are obvious. The DDHF calculations predict differences between the proton (p) and mass (m) moments which are somewhat smaller than we observe. They agree in sign with our findings for ^{154}Sm , but disagree in sign for ^{232}Th . On the other hand, the SSCM result¹⁷ for ^{232}Th reproduces the observed trend in the mass and charge moments both for $\lambda=2$ and for $\lambda=4$, although the absolute values are too large. Our result is, however, in pronounced contrast to a very recent theoretical work,¹⁸ which predicts the deformation of the neutron distribution in actinides to be about twice that of the proton distribution. Obviously, the theoretical situation is not yet settled.

To summarize, we obtain from the systematic analysis of polarized dueteron scattering on the basis of a global optical potential isoscalar transition rates, which are in full agreement with the corresponding electromagnetic values for ^{208}Pb

and the $T=0$ sd -shell nuclei, if the density dependence of the effective nucleon-nucleon interaction is taken into account. This meets theoretical constraints and provides a test of our procedure. For the semimagic nucleus ^{144}Sm we observe a considerably smaller value for the quadrupole transition in accordance with the theoretical prediction. Also for $^{152,154}\text{Sm}$ and ^{232}Th our results for the mass quadrupole moments are considerably smaller than the charge moments. Since the collective model should be most appropriate for the description of these strongly deformed nuclei, it is quite surprising that we observe deviations between charge and mass moments. Certainly further experimental and theoretical work is needed to study these phenomena in more detail.

This work was supported in part by the Deutsches Bundesministerium für Forschung und Technologie. One of us (S.T.H.) is a Max-Planck fellow from the Institute of Atomic Energy, Peking, People's Republic of China.

^(a)Permanent address: Technische Universität München, D-8046 Garching, West Germany.

¹See, e.g., R. Hofmann, thesis, University of Mainz, 1980 (unpublished).

²A. M. Bernstein, V. R. Brown, and V. A. Madsen, Phys. Lett. **103B**, 255 (1981), and Phys. Rev. Lett. **42**, 425 (1979).

³H. Clement, R. Frick, G. Graw, F. Merz, P. Schiemenz, N. Seichert, and Sun Tsu Hsun, Phys. Rev. Lett.

45, 599 (1980).

⁴J. Raynal, Centre d'Etudes Nucléaires, code ECIS 79.

⁵W. E. Daehnick, J. D. Childs, and Z. Vrcelj, Phys. Rev. C **21**, 2253 (1980). As a result of the channel coupling the depths of the real and imaginary central parts have been adjusted systematically (V about 2% larger and W about 10% smaller).

⁶N. Austern, in *Direct Nuclear Reaction Theories*, edited by R. E. Marshak (Wiley, New York, 1970), p. 111 ff, and references quoted therein.

⁷H. Clement *et al.*, to be published. See also, *Polarization Phenomena in Nuclear Physics—1980*, edited by G. G. Ohlsen, AIP Conference Proceedings No. 69 (American Institute of Physics, New York, 1981), p. 576, and Ref. 3.

⁸R. S. Mackintosh, Nucl. Phys. **A245**, 255 (1975).

⁹See Nucl. Data Tables **23**, 3, 547 (1979) and **26**, 47 (1981), and Nucl. Data, Sect. B **5**, 243 (1971), and Nucl. Data Sheets **20**, 165 (1977), and **26**, 281 (1979), and **30**, 1 (1980).

¹⁰R. S. Mackintosh, Nucl. Phys. **A266**, 379 (1976).

¹¹W. D. Meyers, Nucl. Phys. **A204**, 465 (1973); J. P. Jeukenne, A. Lejeune, and C. Mahaux, Phys. Rev. C **16**, 80 (1977).

¹²See, e.g., J. Wambach, F. Osterfeld, J. Speth, and V. A. Madsen, Nucl. Phys. **A324**, 77 (1979).

¹³G. Perrin *et al.*, Nucl. Phys. **A282**, 221 (1977); J. M. Lohr and W. Haeberli, Nucl. Phys. **A232**, 381 (1974).

¹⁴R. J. Powers *et al.*, Nucl. Phys. **A316**, 295 (1979).

¹⁵J. W. Negele and G. Rinker, Phys. Rev. C **19**, 1499 (1979), and King *et al.*, Phys. Rev. C **20**, 2084 (1979).

¹⁶U. Götze, H. C. Pauli, K. Alder, and K. Junkers, Nucl. Phys. **A192**, 1 (1972).

¹⁷M. Brack, T. Ledergerber, H. C. Pauli, and A. S. Jensen, Nucl. Phys. **A234**, 185 (1974).

¹⁸M. Seiwert, P. O. Hess, J. A. Maruhn, and W. Greiner, Phys. Rev. C **23**, 2335 (1981).